Colloids and Surfaces A: Physicochem. Eng. Aspects 453 (2014) 1–6

Contents lists available at ScienceDirect

Colloids and Surfaces A: Physicochemical and Engineering Aspects

journal homepage: www.elsevier.com/locate/colsurfa

Evaporation-driven self-organization of photoluminescent organic dye-doped silica-poly(vinylpyrrolidone) hybrid films prepared by low-speed dip-coating

Hiroaki Uchiyama*, Ryosuke Sasaki, Hiromitsu Kozuka

Department of Chemistry and Materials Engineering, Kansai University, 3-3-35 Yamate-cho, Suita 564-8680, Japan

HIGHLIGHTS

- Sol–gel films containing rhordamine 6G were obtained by low-speed dip-coating.
- Linear stripe patterns were spontaneously formed on the surface of the films.
- The pattern size depended on the solvent contents in the coating solutions.
- The patterned films exhibited light emission only at the surface patterns.

GRAPHICAL ABSTRACT

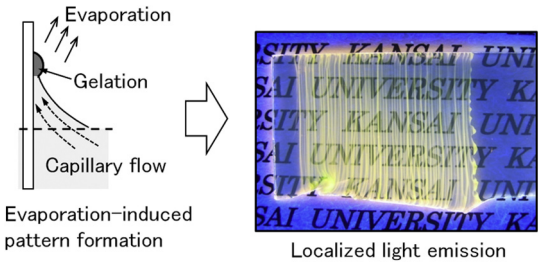

ARTICLE INFO

Article history:
Received 17 January 2014
Received in revised form 11 March 2014
Accepted 21 March 2014
Available online 31 March 2014

Keywords:
Sol–gel coating films
Dip-coating
Surface patterns
Self-organization

ABSTRACT

We prepared silica-poly(vinylpyrrolidone) (PVP) hybrid films containing a photoluminescent organic dye, rhordamine 6G (R6G), by low-speed dip-coating, where the spontaneous pattern formation was induced in the films. Stripe patterns arranged perpendicular to the substrate withdrawal direction were spontaneously formed by stick-slip motion at the meniscus during dip-coating, and the film structure (i.e., the film thickness, and the height, width and spacing of stripe patterns) was changed with increasing amounts of volatile solvent (C_2H_5OH) in solutions ($C_2H_5OH/Si(OCH_3)_4$ mole ratio (x) = 20–150). As a result of the optimization of the film structure, localized photoluminescence at the stripe patterns was achieved over x = 120.

1. Introduction

Evaporation-driven self-assembly and self-organization are attracting much attention as novel fabrication processes of highly-ordered surface patterns on thin films. Solvent evaporation from solutions containing nonvolatile solutes (e.g., colloidal solutions, suspensions and polymer solutions) on a substrate often induces the spontaneous formation of micrometer- and nanometer-scaled surface patterns consisting of the solutes by the convective flow [1–17]. "Stick-slip motion", which is also called as "coffee-ring effect", is widely known as one of typical self-assembly and self-organization processes that are triggered by solvent evaporation [18–24]. When a droplet of solutions containing nonvolatile solutes dries on a substrate, a stripe-like deposit of the solutes is left along the perimeter. The evaporative loss of the solvent at the perimeter provides the outward convective flow of the solutions, resulting in the formation of stripe patterns of the solutes on the substrate. Such pattern formation based on coffee-ring effect can be found in many coating processes for preparing thin films [25–32].

* Corresponding author at: Department of Chemistry and Materials Engineering, Kansai University, 3-3-35 Yamate-cho, Suita 564-8680, Japan.
Tel.: +81 6 6368 1121x5638; fax: +81 6 6388 8797.
E-mail address: h_uchi@kansai-u.ac.jp (H. Uchiyama).

http://dx.doi.org/10.1016/j.colsurfa.2014.03.066
0927-7757/

Table 1
Compositions and viscosity of the coating solutions.

Mole ratio					[R6G] in C_2H_5OH/mM	Viscosity/mPa s
TMOS	C_2H_5OH (x)	H_2O	HNO_3	PVP		
1	20	2	0.01	0.5	0.1	38.0
1	50	2	0.01	0.5	0.1	9.3
1	80	2	0.01	0.5	0.1	5.3
1	100	2	0.01	0.5	0.1	4.2
1	120	2	0.01	0.5	0.1	3.5
1	150	2	0.01	0.5	0.1	2.7

Gel films were deposited on silica glass substrate (20 mm × 40 mm × 0.85 mm) using a dip-coater (PORTABLE DIP COATER DT-0001, SDI, Kyoto, Japan), where the substrates were withdrawn at 0.05 cm min^{-1}. After the deposition, the thin films were kept at room temperature for 24 h in the ambient atmosphere.

In the case of dip-coating process, where the substrate is dipped into the coating solution and then vertically withdrawn at constant speeds, stick-slip motion periodically occurs at the edge of the meniscus during dip-coating, leading to the formation of linear stripe patterns along the surface of coating solution. Such evaporation-driven pattern formation on dip-coating films has been reported in several types of solutions such as suspensions of nanoparticles [33–35] and nanowires [36–38], colloidal solutions [39–42] and polymer solutions [43,44]. Previously, we have investigated the pattern formation induced by stick-slip motion for sol–gel dip-coating films, and found that micrometer-scaled stripe patterns are spontaneously formed on the surface of the films at extremely low substrate withdrawal speeds below 1.0 cm min^{-1} [45,46]. The stripe patterns were arranged perpendicular to the substrate withdrawal direction, and the height and width of the stripes increased with decreasing withdrawal speeds [45] and with increasing coating temperature (i.e., the temperature of substrates, solutions and atmosphere) [46]. Such arranged stripe patterns on sol–gel-derived metal oxide films hold great promise for the application to photonic devices such as diffraction gratings and microlens arrays. Moreover, the addition of luminescent, magnetic, catalytic, and electrically-conductive molecules into the patterned sol–gel films would allow us to immobilize and localize those functional molecules in the patterns, resulting in locally-functionalized thin films.

In this work, we prepared silica-poly(vinylpyrrolidone) (PVP) hybrid films containing a photoluminescent organic molecule, rhordamine 6G (R6G), by low-speed dip-coating, and addressed the introduction of highly-ordered surface patterns into the photoluminescent thin films. The linearly-arranged stripe patterns that are created by stick-slip motion would provide the R6G-doped silica-PVP films with a localized photoluminescence property. In order to develop light emission only at the stripe patterns, the film structure (i.e., the film thickness, and the height, width and spacing of stripe patterns) need to be strictly controlled. Here, we controlled the thickness of the films and the size of the surface patterns by changing the amounts of volatile solvent (C_2H_5OH) in solutions, and optimized the film structure for the localized photoluminescence at the stripe patterns.

2. Experimental

2.1. Materials

The starting materials were tetramethyl orthosilicate ($Si(OCH_3)_4$, TMOS) (Shin-Etsu Silicones, Tokyo, Japan), nitric acid (69 mass%, Wako Pure Chemical Industries, Osaka, Japan), ethanol (C_2H_5OH) (Wako Pure Chemical Industries), PVP (K90, 6.3×10^5 in viscosity average molecular weight, Tokyo Kasei Kogyo Co., Tokyo, Japan), and R6G (Wako Pure Chemical Industries, Osaka, Japan).

2.2. Preparation of R6G-doped silica-PVP hybrid films

At first, R6G was dissolved in C_2H_5OH with stirring at room temperature. The solution containing C_2H_5OH and R6G ([R6G] = 0.1 mM) was used as the solvent of starting solutions. The compositions of the starting solutions are listed in Table 1. Starting solutions of molar compositions, TMOS:C_2H_5OH (containing R6G): H_2O:HNO_3:PVP = 1:x (x = 20–150):2:0.01:0.5, were prepared by the following procedure, where x means the mole ratio for C_2H_5OH exclusive of R6G. The mole ratio for PVP was defined for the monomer (polymerizing unit). First, PVP was dissolved in a 3/4 of the prescribed amount of C_2H_5OH containing R6G, and then TMOS was added. Purified water and nitric acid was added into the remaining amount of the solvent, and then the solution containing C_2H_5OH, R6G, purified water and nitric acid was added dropwise to the TMOS-PVP solution under stirring. The solutions were kept

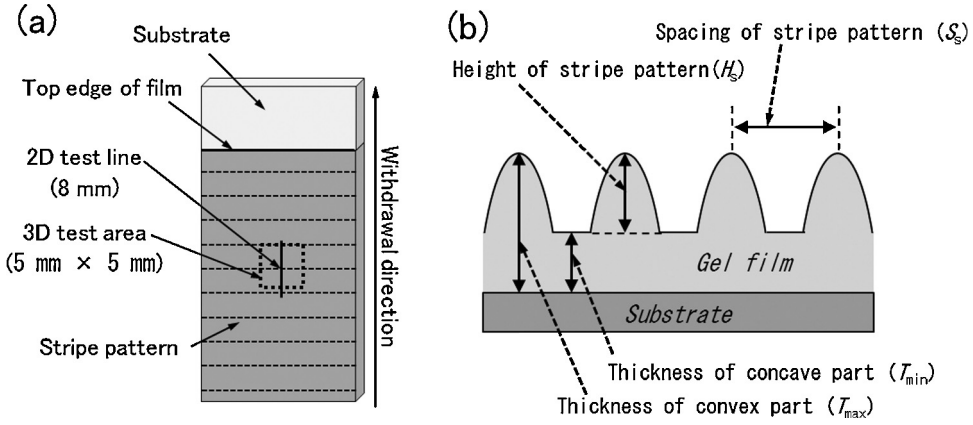

Fig. 1. Schematic illustration of the test line and area employed in 2D and 3D surface roughness measurements (a) and the definition of the film thickness and the height and spacing of surface pattern (b).

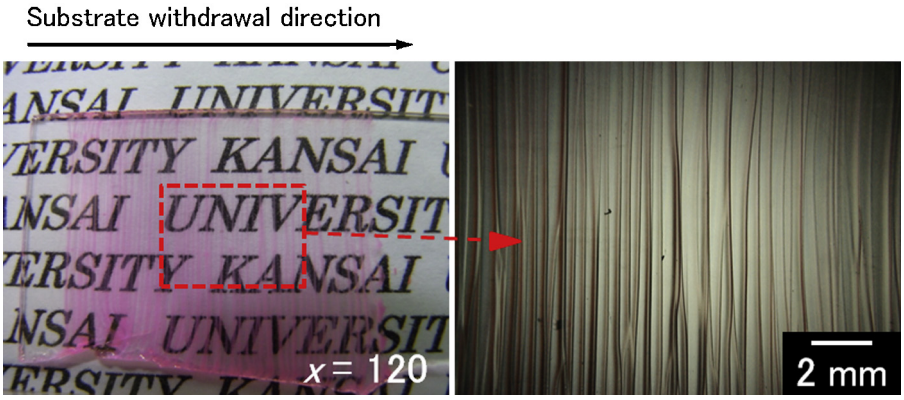

Fig. 2. Typical R6G-doped silica-PVP hybrid films prepared by low-speed dip-coating at 0.05 cm min^{-1}.

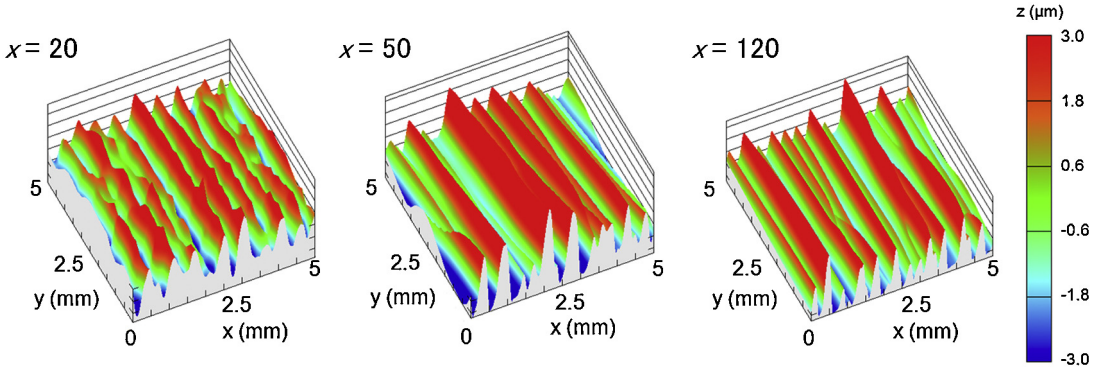

Fig. 3. 3D surface profiles of the R6G-doped silica-PVP hybrid films prepared at x = 20, 50 and 120.

standing at room temperature in a sealed glass container for 30 min, and served as the coating solutions.

2.3. Characterizations

The viscosity of the coating solutions was measured using an oscillating-type viscometer (VM-1G, Yamaichi Electronics, Tokyo, Japan). Microscopic observation was made on the films using an optical microscope (KH-1300, HiROX, Tokyo, Japan). Two- (2D) and three-dimensional (3D) surface profile of the thin films was measured using a contact probe surface profilometer (SE-3500K31, Kosaka Laboratory, Tokyo, Japan). The measurement was conducted at the center of the thin films as shown in Fig. 1a.

The definitions of the film thickness, and the height and spacing of stripe patterns are shown in Fig. 1b. The thickness of the concave (T_{min}) and convex (T_{max}) parts of the patterned films was measured by the surface profilometer. A part of the thin film was scraped off with a surgical knife immediately after the film deposition, and the level difference between the coated part and the scraped part was measured after drying. The height and spacing of stripe patterns were calculated from the 2D surface profiles. Surface roughness parameters, R_Z (ten point height of irregularities) and S (mean spacing of local peaks) represent the

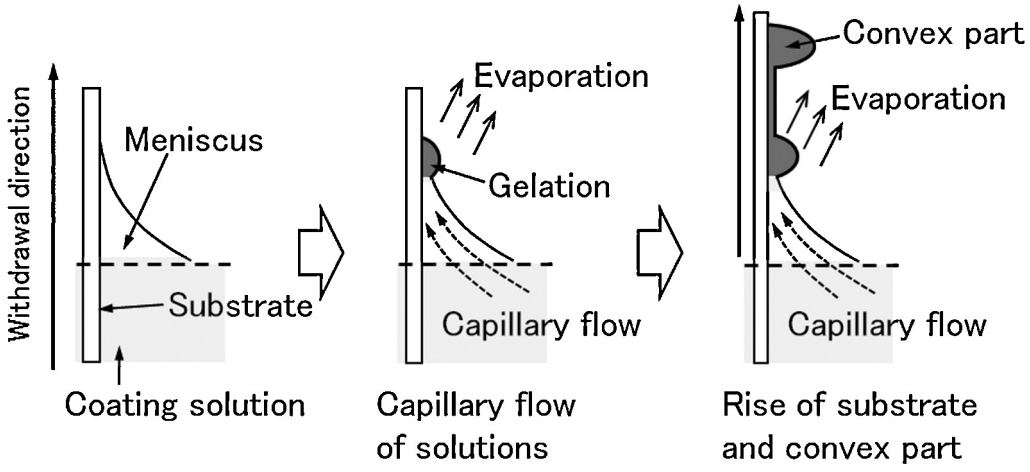

Fig. 4. Schematic illustration of the pattern formation induced by stick-slip motion.

height (H_s) and spacing (S_s), respectively, of the stripe patterns (the definitions of R_Z and S are shown in Supporting Information Figure S1).

The photoluminescence property of the thin films was evaluated by observing the light emission from the films under UV irradiation, where the UV irradiation was conducted by an illuminating equipment (Model EF-280C/J, Spectronics, New York, USA) that radiates 245 nm UV light from two 8 W UV tubes (Model BLE-8T254, Spectronics, New York, USA).

3. Results and discussion

R6G-doped silica-PVP hybrid films were prepared by low-speed dip-coating at 0.05 cm min^{-1} from the coating solutions of various $C_2H_5OH/Si(OCH_3)_4$ mole ratios (x = 20–150). A typical dip-coating film thus obtained is shown in Fig. 2. Transparent, slightly pink thin films were obtained irrespective of the C_2H_5OH contents, x, and stripe patterns arranged perpendicular to the substrate withdrawal direction were visually confirmed on the surface. The pink color at the convex parts of the patterned films was more intense than that at the concave parts. Fig. 3 shows the 3D surface profiles of the R6G-doped silica-PVP hybrid films. Linear stripe patterns of 3.0–6.0 μm in height and 300–500 μm in width were observed for the films, depending on the C_2H_5OH contents, x.

The spontaneous formation of stripe patterns on sol–gel coating films during low-speed dip-coating is attributed to stick-slip motion triggered by solvent evaporation at the meniscus [45,46]. The schematic illustration of the pattern formation is shown in Fig. 4. During the low-speed dip-coating (0.05 cm min^{-1}), the gelation of the coating solution locally progresses at the edge of the meniscus due to the solvent evaporation, and then the coating solutions is raised to the edge of the meniscus by capillary flow [47,48]. As a consequence, the thickness of the coating layer locally increases at the edge of the meniscus, leading to the formation of a convex gel part. The convex part is continuously raised with the substrate withdrawal, and progressively segregated from the meniscus. As a result, the edge of the coating solution drops down like a receding tide until a next gel part forms at the meniscus. Stripe patterns arranged perpendicular to the withdrawal direction are formed through the repetition of the formation of convex gel part at the edge of meniscus.

Fig. 5 shows the dependence of the thickness of concave (T_{min}) and convex (T_{max}) parts, and the height (H_s) and spacing (S_s) of stripe patterns on the $C_2H_5OH/Si(OCH_3)_4$ mole ratio in solutions (x). The thickness of concave (T_{min}) and convex (T_{max}) parts decreased with increasing x (Fig. 5a), which could be caused by the decrease in the concentration of $Si(OCH_3)_4$ and the viscosity of solutions. The large reduction of thickness in the range of x = 20–50 was deduced to be mainly attributed the drastic decrease in the viscosity of solutions (Table 1). In the range of x = 50–150, T_{min} slightly decreased with increasing x (Fig. 5b).

The height of the stripe patterns (H_s) is shown in Fig. 5a, where the H_s almost agreed with the difference between T_{min} and T_{max}. The increase in x from 20 to 50 led to the increase in H_s, while the increase in the C_2H_5OH contents reduced the thickness at the convex parts (T_{max}). The stripes exhibited the maximum height of ca. 6.5 μm at x = 50. The height of stripe patterns is thought to increase with increasing volume of the capillary flow at the meniscus [45–48], where the lower viscosity of solutions due to the higher solvent contents would provide larger flow volume, resulting in the formation of larger stripe patterns. On the other hand, the further increase in x from 50 to 80 led to the decrease in H_s, and then H_s almost unchanged over x = 80. Higher solvent contents increase the fluidity of coating solutions and consequently provide larger stripe patterns, while the decrease in the $Si(OCH_3)_4$ concentration reduces the thickness of the films. The competition between the increase in the solution fluidity and the decrease in the $Si(OCH_3)_4$ concentration could result in the constant H_s in the range of x = 80–150.

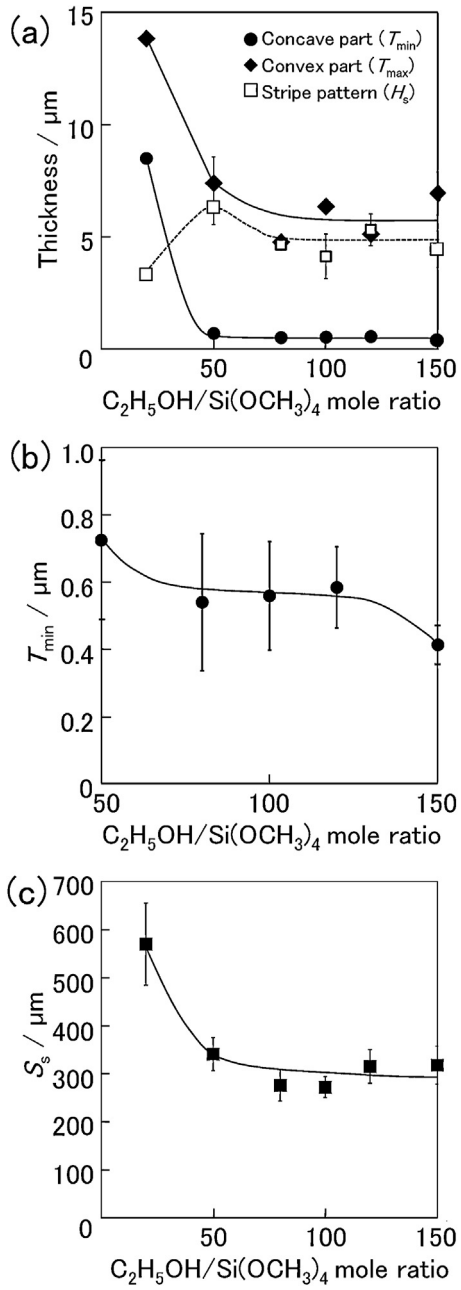

Fig. 5. Dependence of the thickness of the concave (T_{min}) and convex (T_{max}) parts, and the height (H_s) and spacing(S_s) of stripe patterns on the $C_2H_5OH/Si(OCH_3)_4$ mole ratio in the coating solutions (x). (a) The variation in T_{min}, T_{max} and H_s in the rage of x = 20–150, (b) T_{min} of x = 50–150, and (c) S_s of x = 20–150.

The spacing of the stripe patterns (S_s) drastically decreased with increasing x from 20 to 50, and almost unchanged over x = 50 (Fig. 5c). Fig. 6 shows the 2D surface profiles of the hybrid films. The surface profiles indicate that the stripe patterns become sharper with increasing x. As mentioned above, in the case of stick-slip motion on sol–gel films, a convex gel part segregates from the meniscus of solutions with the substrate withdrawal, leading to the formation of periodic stripe patterns [45,46]. The increase in the solvent contents reduces the viscosity of solutions and thus the convex part is deduced to more smoothly segregate from the

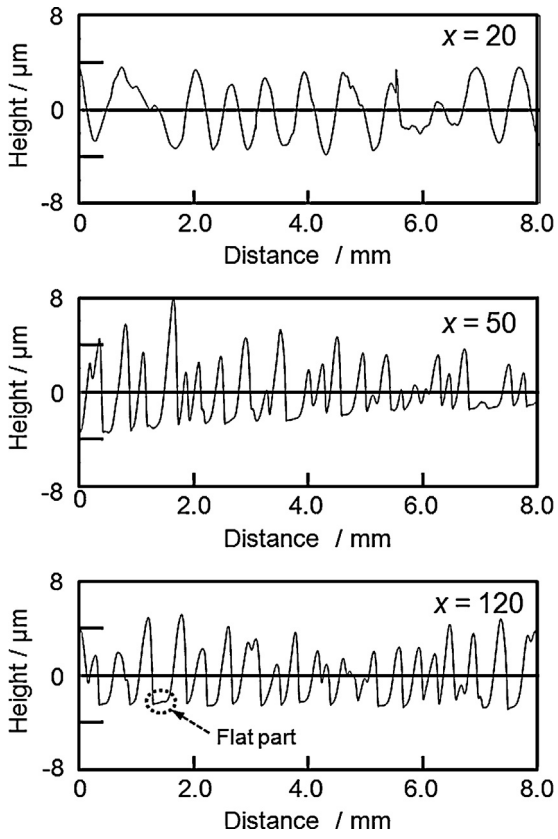

Fig. 6. 2D surface profiles of the R6G-doped silica-PVP hybrid films prepared at $x = 20$, 50 and 120.

meniscus, which could result in the formation of sharp stripe patterns. Moreover, the 2D surface profiles also indicate that the flat parts of 100–300 μm in width appeared between the convex parts over $x = 50$ (Fig. 6). Since the viscosity of solutions over $x = 50$ is very low, the edge of solution drastically drops after the segregation of convex gel part from the meniscus, and then the flat parts could be formed between the stripe patterns.

Fig. 7 shows the light emission from the hybrid films under UV irradiation. The photoluminescence intensity at the concave parts of the films obviously decreased with increasing x, and the patterned films prepared over $x = 120$ exhibited light emission only at the convex parts. Although photoluminescence molecules are thought to be contained in both the convex and concave parts irrespective of x, the localized light emission was achieved over $x = 120$, which could be attributed to the smaller thickness of concave parts and the presence of the flat parts between the convex parts. The thickness of the concave parts (T_{min}) slightly decreased with increasing x from 50 to 120 (Fig. 5b), resulting in the reduction in the photoluminescence intensity at the concave parts. Moreover, the distance between the convex parts increased and the flat parts appeared with increasing x (Fig. 6), which could enhance the contrast of the light emission on the hybrid films. As a result, the localized light emission could be developed only at the convex parts. Moreover, in the present case, the R6G/$Si(OCH_3)_4$ mole ratio was not constant ([R6G] in $C_2H_5OH = 0.1$ mM), and the amount of R6G in the silica-PVP hybrid films increased with increasing x. We have also prepared the R6G-doped silica-PVP hybrid films from the coating solutions of $x = 50$ and 120 with a constant R6G/$Si(OCH_3)_4$ mole ratio, and confirmed that the localized light emission is observed only at $x = 120$ as well as in the present case (Supporting information Table S1–S2 and Figure S2). Thus, the pattern size

Fig. 7. Light emission from the R6G-doped silica-PVP hybrid films prepared at $x = 20$, 50 and 120 under UV irradiation.

and shape could be more important for the localized light emission than the amount of R6G in the films.

4. Conclusion

Micron-scaled linear stripe patterns arranged perpendicular to the substrate withdrawal direction were formed on R6G-doped silica-PVP hybrid films prepared by low-speed dip-coating at 0.05 cm min^{-1}. The stripe patterns were created by stick-slip motion at the meniscus of coating solutions during dip-coating, and the size and shape of the patterns depended on the $C_2H_5OH/Si(OCH_3)_4$ mole ratio in solutions (x). The thickness of the concave and convex parts of the patterned films decreased with increasing solvent contents. The height of the stripe patterns increased with increasing x from 20 to 50, and the further increase in x reduced the height. The stripe patterns became sharper and the distance between the convex parts increased with increasing x. The variation in the size and shape of the stripe patterns could

be caused by the competition between the increase in the fluidity of solutions and the decrease in the $Si(OCH_3)_4$ concentration with increasing solvent contents. Localized photoluminescence at the convex parts was achieved in the patterned films by the optimization of the film structure (i.e., the film thickness, and the height, width and spacing of stripe patterns).

Acknowledgments

This work was supported by JSPS KAKENHI Grant-in-Aid for Young Scientists (B) Grant Number 24760554.

Appendix A. Supplementary data

Supplementary data associated with this article can be found, in the online version, at http://dx.doi.org/10.1016/j.colsurfa.2014.03.066.

References

[1] E. Bormashenko, R. Pogreb, O. Stanevsky, Y. Bormashenko, T. Stein, O. Gengelman, Langmuir 21 (2005) 9604.
[2] S.W. Hong, J. Wang, Z.Q. Lin, Angew. Chem. Int. Ed. 48 (2009) 8356.
[3] J.A. Lim, W.H. Lee, H.S. Lee, J.H. Lee, Y.D. Park, K. Cho, Adv. Funct. Mater. 18 (2008) 229.
[4] L. Malfatti, Y. Tokudome, K. Okada, S. Yagi, M. Takahashi, P. Innocenzi, Microporous Mesoporous Mater. 163 (2012) 356.
[5] A. Mihi, M. Ocana, H. Miguez, Adv. Mater. 18 (2006) 2244.
[6] B.Q. Sun, H. Sirringhaus, J. Am. Chem. Soc. 128 (2006) 16231.
[7] M. Takahashi, C. Figus, L. Malfatti, Y. Tokuda, K. Yamamoto, T. Yoko, T. Kitanaga, Y. Tokudome, P. Innocenzi, NPG Asia Mater. 4 (2012) e22.
[8] H. Uchiyama, Y. Mantani, H. Kozuka, Langmuir 28 (2012) 10177.
[9] L.K. Wang, Y. Wan, Y.Q. Li, Z.Y. Cai, H.L. Li, X.S. Zhao, Q. Li, Langmuir 25 (2009) 6753.
[10] S. Wong, V. Kitaev, G.A. Ozin, J. Am. Chem. Soc. 125 (2003) 15589.
[11] K.H. Wu, S.Y. Lu, H.L. Chen, Y.Y. Chen, Macromol. Chem. Phys. 209 (2008) 615.
[12] H. Yabu, M. Shimomura, Adv. Funct. Mater. 15 (2005) 575.
[13] M. Yoldi, C. Arcos, B.R. Paulke, R. Sirera, W. Gonzalez-Vinas, E. Gornitz, Mater. Sci. Eng. C 28 (2008) 1038.
[14] H. Uchiyama, W. Namba, H. Kozuka, Langmuir 26 (2010) 11479.
[15] C. Farcau, H. Moreira, B. Viallet, J. Grisolia, L. Ressier, ACS Nano 4 (2010) 7275.
[16] J.X. Huang, F. Kim, A.R. Tao, S. Connor, P.D. Yang, Nat. Mater. 4 (2005) 896.
[17] B. Li, W. Han, M. Byun, L. Zhu, Q. Zou, Z. Lin, ACS Nano 7 (2013) 4326.
[18] R.D. Deegan, O. Bakajin, T.F. Dupont, G. Huber, S.R. Nagel, T.A. Witten, Nature 389 (1997) 827.
[19] R.D. Deegan, O. Bakajin, T.F. Dupont, G. Huber, S.R. Nagel, T.A. Witten, Phys. Rev. E 62 (2000) 756.
[20] H. Hu, R.G. Larson, J. Phys. Chem. B 110 (2006) 7090.
[21] P. Innocenzi, L. Malfatti, M. Piccinini, D. Grosso, A. Marcelli, Anal. Chem. 81 (2009) 551.
[22] W.D. Ristenpart, P.G. Kim, C. Domingues, J. Wan, H.A. Stone, Phys. Rev. Lett. 99 (2007) 234502.
[23] T. Still, P.J. Yunker, A.G. Yodh, Langmuir 28 (2012) 4984.
[24] H.S. Kim, C.H. Lee, P.K. Sudeep, T. Emrick, A.J. Crosby, Adv. Mater. 22 (2010) 4600.
[25] S. Choi, S. Stassi, A.P. Pisano, T.I. Zohdi, Langmuir 26 (2010) 11690.
[26] W. Han, Z. Lin, Angew. Chem. Int. Ed. 51 (2012) 1534.
[27] M. Byun, W. Han, B. Li, X. Xin, Z. Lin, Angew. Chem. Int. Ed. 52 (2013) 1122.
[28] W. Han, M. Byun, B. Li, X. Pang, Z. Lin, Angew. Chem. Int. Ed. 51 (2012) 12588.
[29] W. Han, M. He, M. Byun, B. Li, Z. Lin, Angew. Chem. Int. Ed. 52 (2013) 2564.
[30] D. Kim, S. Jeong, B.K. Park, J. Moon, Appl. Phys. Lett. 89 (2006) 264101.
[31] H.M. Ma, R. Dong, J.D. Van Horn, J.C. Hao, Chem. Commun. 47 (2011) 2047.
[32] J. Xu, J.F. Xia, Z.Q. Lin, Angew. Chem. Int. Ed. 46 (2007) 1860.
[33] U. Olgun, V. Sevinc, Powder Technol. 183 (2008) 207.
[34] S. Watanabe, K. Inukai, S. Mizuta, M.T. Miyahara, Langmuir 25 (2009) 7287.
[35] S. Watanabe, Y. Mino, Y. Ichikawa, M.T. Miyahara, Langmuir 28 (2012) 12982.
[36] J.X. Huang, R. Fan, S. Connor, P.D. Yang, Angew. Chem. Int. Ed. 46 (2007) 2414.
[37] N.L. Liu, Y. Zhou, L. Wang, J.B. Peng, J.A. Wang, J.A. Pei, Y. Cao, Langmuir 25 (2009) 665.
[38] C.Y. Zhang, X.J. Zhang, X.H. Zhang, X. Fan, J.S. Jie, J.C. Chang, C.S. Lee, W.J. Zhang, S.T. Lee, Adv. Mater. 20 (2008) 1716.
[39] H. Bodiguel, F. Doumenc, B. Guerrier, Langmuir 26 (2010) 10758.
[40] M. Ghosh, F.Q. Fan, K.J. Stebe, Langmuir 23 (2007) 2180.
[41] Y. Mino, S. Watanabe, M.T. Miyahara, Langmuir 27 (2011) 5290.
[42] Y. Mino, S. Watanabe, M.T. Miyahara, ACS Appl. Mater. Interfaces 4 (2012) 3184.
[43] J. Jang, S. Nam, K. Im, J. Hur, S.N. Cha, J. Kim, H.B. Son, H. Suh, M.A. Loth, J.E. Anthony, J.J. Park, C.E. Park, J.M. Kim, K. Kim, Adv. Funct. Mater. 22 (2012) 1005.
[44] G. Pu, S.J. Severtson, Langmuir 24 (2008) 4685.
[45] H. Uchiyama, M. Hayashi, H. Kozuka, RSC Adv. 2 (2012) 467.
[46] H. Uchiyama, D. Shimaoka, H. Kozuka, Soft Matter 8 (2012) 11318.
[47] M. Faustini, B. Louis, P.A. Albouy, M. Kuemmel, D. Grosso, J. Phys. Chem. C 114 (2010) 7637.
[48] D. Grosso, J. Mater. Chem. 21 (2011) 17033.